Innovative process for precise grinding of optical free-form elements

Jinst

Published by IOP Publishing for Sissa Medialab

Received: *December 19, 2022*
Revised: *February 28, 2023*
Accepted: *March 22, 2023*
Published: *April 13, 2023*

Innovative process for precise grinding of optical free-form elements

František Procháska,[a,*] **David Tomka,**[a] **Petr Vavruška,**[b] **Markéta Paprčková,**[a] **Radek Melich,**[a] **Ondřej Matoušek**[c] **and Emilie Lhomé**[d]

[a] *Institute of Plasma Physics of the Czech Academy of Sciences, Za Slovankou 1782/3, Prague 8, Liben, 182 00 Czech Republic*
[b] *Czech Technical University in Prague, Faculty of Mechanical Engineering, Department of Production Machines and Equipment, Horská 3, Prague 2, 128 00 Czech Republic*
[c] *asphericon s.r.o., Milířská 449, Jeřmanice, 463 12 Czech Republic*
[d] *European Space Agency — ESTEC, Keplerlaan 1, Noordwijk, 2200 AG The Netherlands*

E-mail: prochaska@ipp.ca.cz

Abstract: The aim of the presented article is to share experience gained throughout the course of two projects focused on precise grinding of a free-form glass optical element with the objective of achieving a surface shape error of less than approximately 10 µm PV before the subsequent polishing phases. Compared to spheres or aspheres machining, it is considerably more demanding, mainly due to the impossibility of using rotationally symmetric shape corrections. The developed and tested process combines a mechanical engineering approach based on the use of the current Computer Aided Design and Computer Aided Manufacturing software with their respective strengths and weaknesses and an optical engineering approach, for which the employment of CNC machines featuring precise control but low flexibility is typical. Therefore, attention is paid mainly to the description of particular process steps like CAD construction and CNC grinding step programming with regard to the necessary software and data handling, as well as the required parametrisation of the used machine equipment.

Keywords: Optics; Space instrumentation

*Corresponding author.

https://doi.org/10.1088/1748-0221/18/04/P04022

2023 JINST 18 P04022

Contents

2023 JINST 18 P04022

1 Introduction

In recent years, with the boom in the development of high-precision machining processes for aspheric optics, precision machining of free-form optics has been gaining ground. This is caused, on the one hand, by the development of design software capabilities and, on the other hand, by the development of precise measuring methods which, alongside precise Computer Numerical Control (CNC) grinding and polishing machinery, form an important part of the process chain. In any case, proper grinding of the material is one of the crucial processes in optical manufacturing because it determines the quality of the surface with respect to the polishing used. Furthermore, the duration of the polishing cycle can be dramatically reduced by the use of proper grinding techniques [1].

During precise optical surface grinding which requires the precision of the shape in units of microns, the process is generally divided into three steps [2]. In the first step, a best-fit sphere (BFS) radius is generated using a standard spherical full-surface cup-tool technology. In this step, the bulk of the material is removed. In the next steps of coarse and fine grinding, wheel-tools are used for the sub-aperture grinding of the element shape. During coarse grinding, the difference between the BFS and the demanded shape is removed. In the fine grinding phase, a layer of the material is eliminated in several grinding cycles to reduce the surface roughness and the subsurface damage, and the element shape error is minimized using the tool path correction method. In this step, a suitable surface form for the polishing process is prepared. Especially in free-form grinding, where 3-axis and 5-axis CNC machines are most widely used, the path definition of the correctly selected grinding tool with regards to its shape and acceleration control plays a very important role. Besides traditional methods of the tool path definition, such as direction parallel path, contour parallel path,

or spiral path, another method, called space-filling curves, can be used but the appropriate setting of the tool path parameters is always essential [3].

1.1 CAD/CAM machinery

In contrast to the optical sector, in the field of precision mechanical engineering implemented across a wide range of industries, Computer Aided Design (CAD) and Computer Aided Manufacturing (CAM) have nowadays become the basis of the process chain of highly productive and repeatable manufacturing. While CAD enables efficient and precise construction of 2D or 3D geometric models of parts, the CAM software uses these models as the basis for programming 3-axis and 5-axis CNC machining processes [4]. With regard to the geometry of a part, the CAM software can create machining strategies as well as define tool paths and the necessary process parameters, which are subsequently transformed according to the ISO 6983 standard [5] using a post-processor into the form of the final G-code controlling a specific CNC device. Thanks to this approach, it is then possible, among other things, to accurately simulate and optimize the machining process, for example, in order to define suitable process blocks and to eliminate repetitive steps [6], which results in a more efficient production process. CAD/CAM machines also feature special functions to perform 3D shape correction, thus minimizing shape deviation of the realized part from the designed nominal shape.

1.2 Specific features of free-form machining

With regard to the above-mentioned, the 3D element model usage in the process chain is beneficial for free-form machining. Its precision, often up to nanometer level, is a crucial requirement for successful realization. At the same time, the final form of the 3D model often depends on the procedure of its construction, usually executed in a 3D CAD software, and it is, therefore, necessary to define this procedure (character of entities, order of their placement, bonding, axes orientation, tilting, etc.) in detail [7].

As surface shape measurement is fundamental to precise machining, measurement technology limits the surfaces that can be effectively manufactured and further determines which surfaces can be cost-effectively employed in optical designs. Free-form optical surfaces are advantageous for optical designers since they provide additional degrees of freedom for optimization. However, the loss of symmetry and increase in the number of degrees of freedom make the measurement of free-forms more challenging. Currently, there exist several measuring techniques, such as the null test computer-generated holograms (CGHs), variable optical null interferometry [8], or optical single-point probing profilometry [9], which are suitable for free-form measurement.

A very important aspect that also complicates the machining process setup is the wide range of free-form shape definition options as well as the need to select a referencing system whose choice has to be subsequently maintained throughout the whole machining chain. Theoretically, there exist many options like using a data cloud, orthogonal polynomials, NURBS, etc. [10, 11]; however, the appropriate selection would be determined by the software available for free-form element construction and subsequent data handling, as well as by the requirements for free-form shape capture precision.

Regarding the reference system, special attention must be paid to the right orientation of all free-form element axes, machining programming axes, as well as machine axes. For this purpose,

2023 JINST 18 P04022

the use of datum surfaces on a free-form element is necessary. Data handling (data modification and formatting) must then be performed in such a way as to ensure the correct and accurate transmission of all the contained information concerning both the shape of the free-form element and the machining process [12].

However, in connection with the production of high-precision glass free-form optics for demanding applications such as laser or spectrometric devices, the question arises whether the common limit value of shape accuracy of 10 µm required for subsequent polishing is achievable when applying the optical CNC grinding along with the mechanical engineering CAD/CAM machinery. As it is not currently possible to find a clear answer in the literature, we would like to try to answer the question in the presented article based on our performed experiments.

2 Experiment setup

2.1 Free-form element design

The free-form S-BSL7 glass element was designed as an off-axis part of the asphere described in table 1. It is important to emphasize that the surface will be treated as a purely free-form surface, where there is no coincidence of the free-form optical/mechanical axis with the aspherical surface axis.

Table 1. Parameters of aspheric design.

Material	S-BSL7 glass
Diameter D [mm]	132
Vertex shape	Convex
Vertex radius R [mm]	80
Curvature C = 1/R [mm^{-1}]	0.0125
Conic constant K [—]	0
Aspheric coefficient A6 [—]	-5×10^{-12}
Sag check point at ρ = 50 mm Z(50) [mm]	17.472

Firstly, a mother aspherical surface with a diameter of D = (97/2 + 17.5) × 2 = 132 mm was created in the Zemax software, which was then imported into the CAD software, where the 3D model of the optical free-form element with a diameter of 97 mm was created. An auxiliary axis was constructed at a perpendicular distance to the optical axis of the mother aspherical surface. At the point of intersection of this axis with the surface, a normal was constructed to obtain the mechanical axis of the free-form element (the angle between the optical axis and the mechanical axis is 12.63°; the distance of the intersection of the axes from the surface is 80.02 mm; the centre thickness is 26.3 mm). Finally, the free-form element was rounded at a distance of 48.5 mm from this mechanical axis (figure 1). In accordance with the construction of the free-form model, it was also necessary to create an assembly of the manufacturing and measuring holders to compensate the off-axis shift and tilt (figure 1) enabling the use of shape measurement by a QED Technologies Aspheric Stitching Interferometer (QED ASI).

2023 JINST 18 P04022

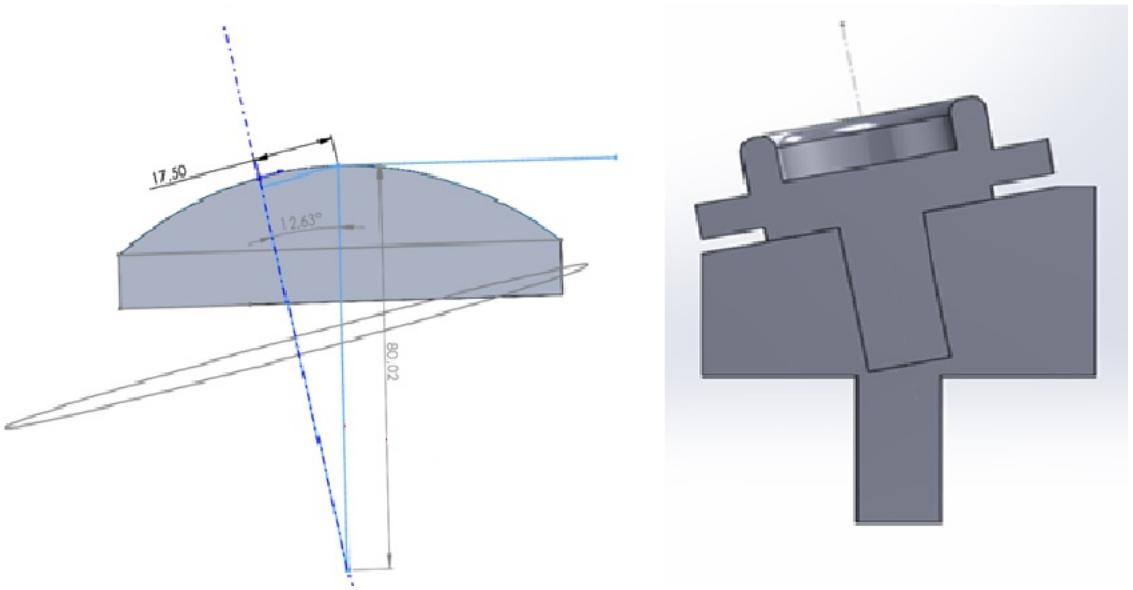

Figure 1. 2D scheme of FF element construction (left) and holder assembly (right): CNC holder at the top, measuring holder at the bottom.

2.2 Free-form CNC grinding

All free-form grinding steps were programmed using the Siemens NX CAD-CAM software for 5-axis machining and a customized post-processor specially developed for free-form machining on the Satisloh SPM 60 machine.

At first, the CAD 3D free-form model was created in the `.step` format and imported into the Siemens NX CAM software, where the origins of the model, machining task, as well as machine coordinate systems were aligned. Then, various machining strategies were simulated and, based on the kinematic possibilities of the Satisloh machine and the simulation results gained, the appropriate strategies were selected.

For the actual grinding, the workpiece glued onto a CNC holder by optical wax was fixed to the machine, centred, and a best-fit radius of 80.33 mm was ground by a cup diamond tool. Then, the workpiece orientation, in accordance with the X; Y axes of the machine axes, was checked by an internal tactile probe. The free-form shape generation was realized by a wheel diamond tool (D90 and D38) in two steps (semi-coarse and fine grinding), each at several grinding cycles for subsurface damage minimization.

For the semi-coarse grinding step, a radial zig strategy combining a linear tool movement between the edge and the centre with the rotary positioning of the workpiece was chosen (see figure 2) because it allowed a more productive way of removing excess material. After the semi-coarse process, for fine and also for corrective grinding, a variable contour strategy with a spiral tool path (figure 3) was employed. This method was used to machine the input surface with an appropriate deviation from the nominal value, with a sufficiently low roughness, and with a mid-spatial frequencies content acceptable for subsequent polishing.

2023 JINST 18 P04022

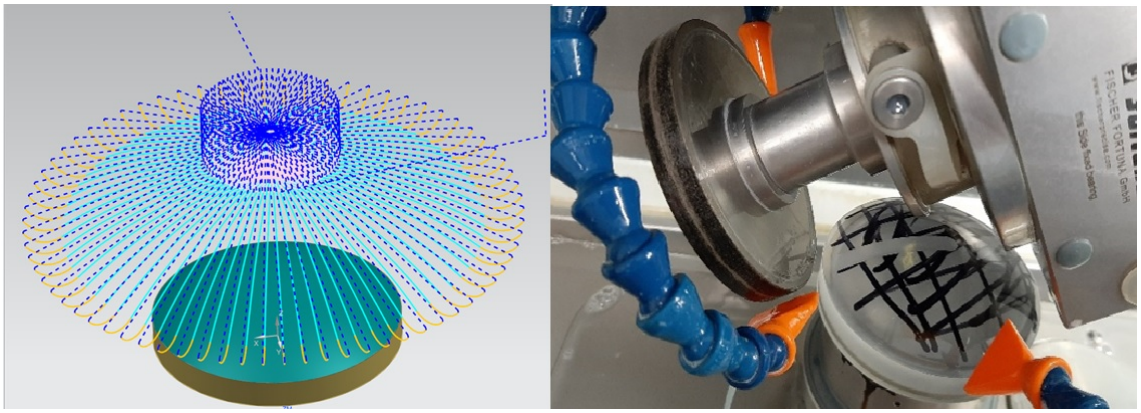

Figure 2. Free-form radial Zig strategy.

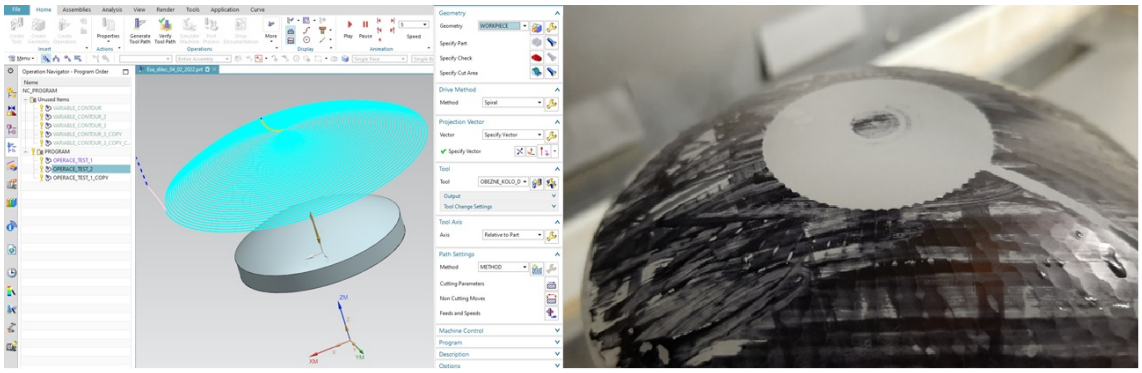

Figure 3. Free-form spiral strategy.

After the free-form fine grinding, the generated surface was quickly pre-polished by CNC raster bonnet polishing and measured by a QED ASI equipped with an assembly of manufacturing and measuring holders.

2.3 Free-form CNC corrective grinding

In general, it can be said that the corrective grinding process proposed is based on the correction of the tool path, which causes a deviation from the desired shape. Such a deviation is mainly due to inaccuracies in the tool geometry input values and results in incorrect positioning of the tool in relation to the workpiece. Therefore, for a proper result of corrective grinding, it is necessary to obtain data describing the shape error of the primary grinding and to convert these data into a form and format that can be processed in the CAM software, which is either a `.stp`, `.step`, or `.prt` file. This file is usually obtained by summing the 3D nominal model and the measured shape error. For this purpose, it is necessary to solve the conversion of the measurement result file `.xyz` to `.ascii` format, and the conversion of the nominal 3D CAD model to the data cloud `.ascii` format with the same number and size of pixels and at the same data centring. The described data processing and their subsequent summing was performed in the MATLAB software by quadratic interpolation and other functions accessible from the MATLAB tool box. Alternatively, it can be done by another appropriate software, such as the Zeeko Metrology Toolkit. The obtained file was imported into

2023 JINST 18 P04022

the CAD software (Siemens NX), where the global deformation function was used. Finally, the resulting global deformation function was imported into the CAM software and the same grinding parameter settings of the tool paths were recalculated and applied.

2.4 CNC grinding and corrective grinding link-up

The process diagram presented in figure 4 shows the link-up of the CNC grinding and the corrective grinding, demonstrating the continuity of the individual steps of the process. Briefly, first the CNC-grinded optical element is measured to determine the shape error and then it is regrinded by corrective grinding based on the global deformation function definition.

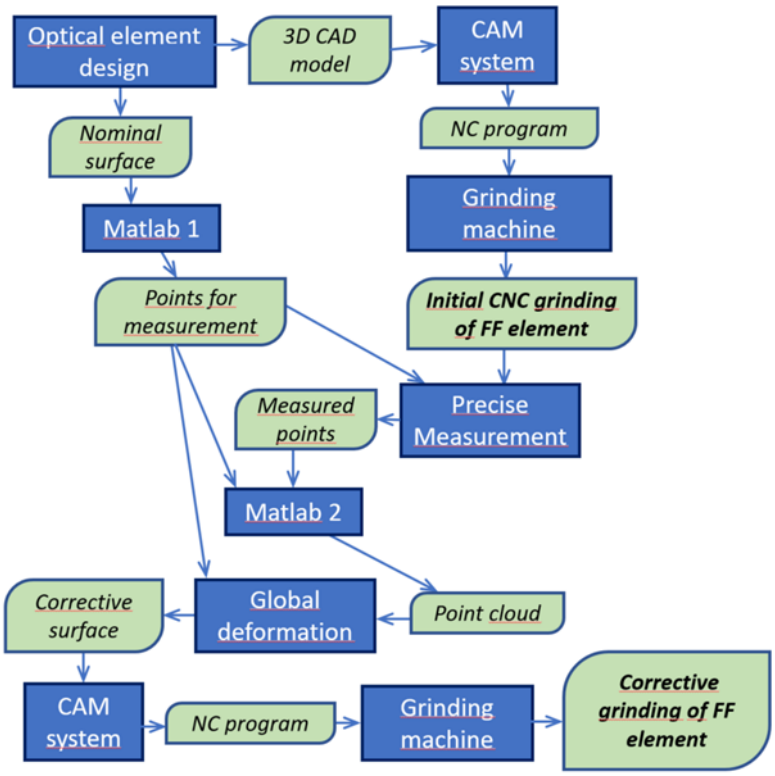

Figure 4. Diagram of the free-form grinding process.

If it is possible to assume that there is no fundamental change in the offsets of the grinding machine or the geometry of the grinding tool, e.g., due to wear, the resulting toolpath for corrective grinding can be used to grind a series of workpieces with the required accuracy.

3 Results and discussions

3.1 Free-form CNC grinding

When the first free-form surface was made from S-BSL7 optical glass after the prepolishing step, sharp, milimetre-sized waves were identified on the surface (figure 5 left), although the basic NXCAM program did not anticipate any difficulties in the realization of the surface. A subsequently

2023 JINST 18 P04022

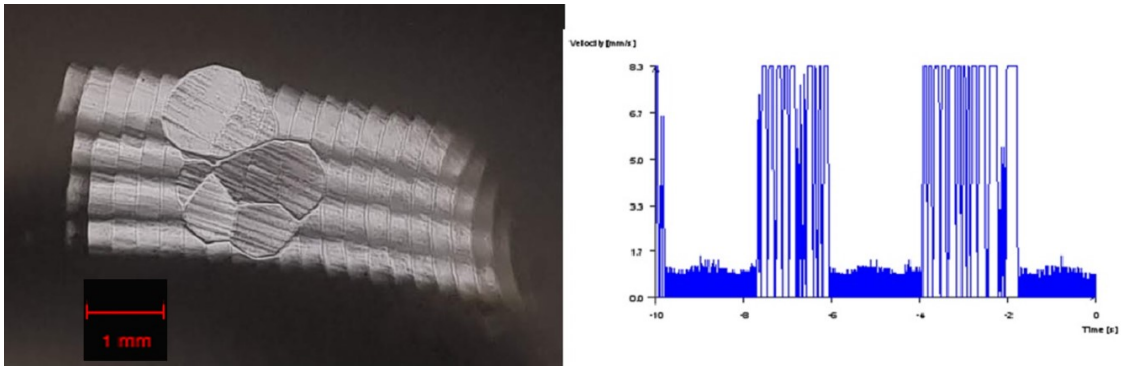

Figure 5. Zoom of the free-form element manufacturing surface (left) and results of the process simulation plotted as tilting axis movement velocity vs. process time (right).

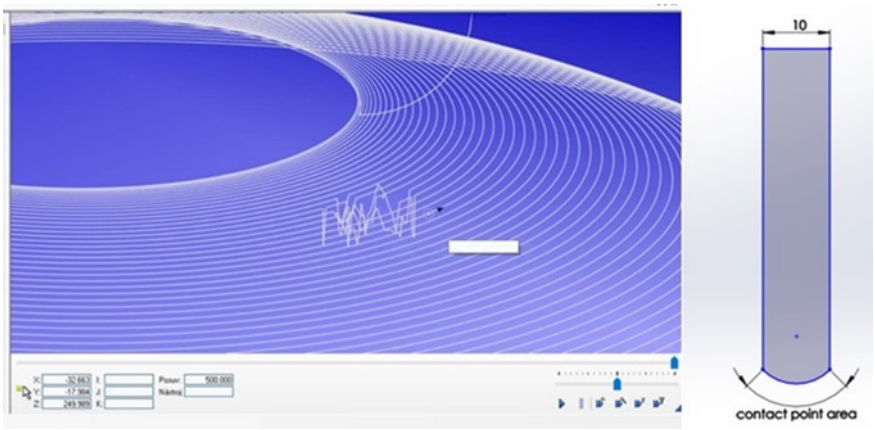

Figure 6. Analysis in the CIMCO program revealing of the tool path disruption (left) caused by rapid contact point movement on the tool surface (right).

processed numerical simulation showed a large change in the tilting axis movement velocity (figure 5 right). Therefore, a detailed analysis was performed using the CIMCO software, where the sharp waves on the toolpath were seen and the issue was identified as the rapid movement of the grinding point across the tool surface (figure 6).

To solve the described issue, it was necessary to define the T-cutter software tool as if its width was close to zero. This was mechanically unrealistic, but it enabled us to eliminate the fast position changes of intersection point between the tool and the free-form element. Subsequently, the CAM software calculation visualized some parasitic tool movements that made high-quality machining impossible on the edge of the free-form element. Another error visualized in CAD/CAM was the tool crossing the free-form element on the last spiral turn, which would cause a collision between the tool and the element, resulting in the destruction of both. These errors had to be manually corrected in the Edit Path menu.

The application of the above-described process resulted in a free-form surface with a shape error (measured by QED ASI after several cycles of raster prepolishing) of around 15 µm PV or 2.5 µm RMS (see figure 7), which was too high for subsequent corrective polishing and achieving the necessary final precision. Thus, corrective grinding was necessary.

2023 JINST 18 P04022

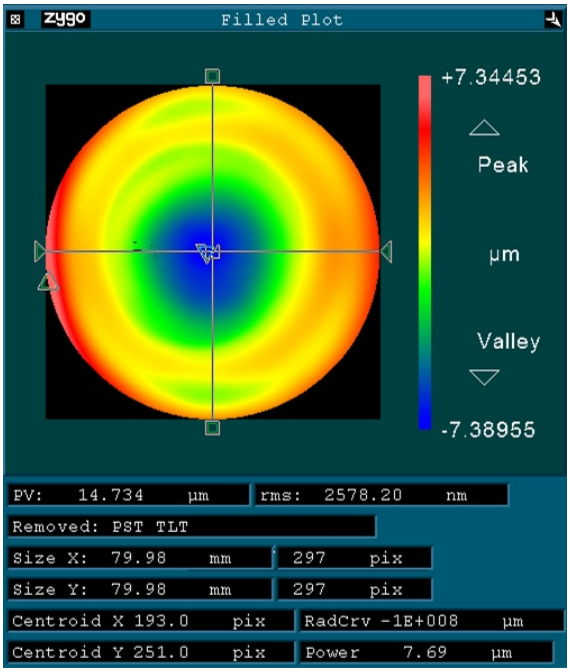

Figure 7. Free-form surface error after CNC grinding and pre-polishing; piston and tilt removed. Results from QED ASI.

3.2 Free-form CNC corrective grinding

To find a suitable setting of the global deformation function parameters (figure 8), a process simulation was conducted to monitor the overall changes in curvature and shape deviation in certain sections of the free-form element, and an effort was made to optimize them (figure 9).

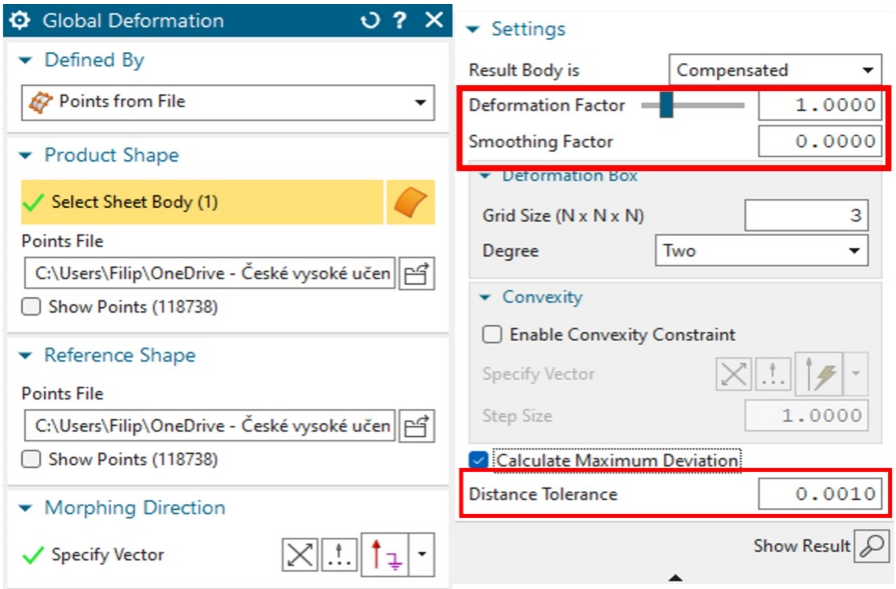

Figure 8. Global deformation function settings with tested parameters marked.

2023 JINST 18 P04022

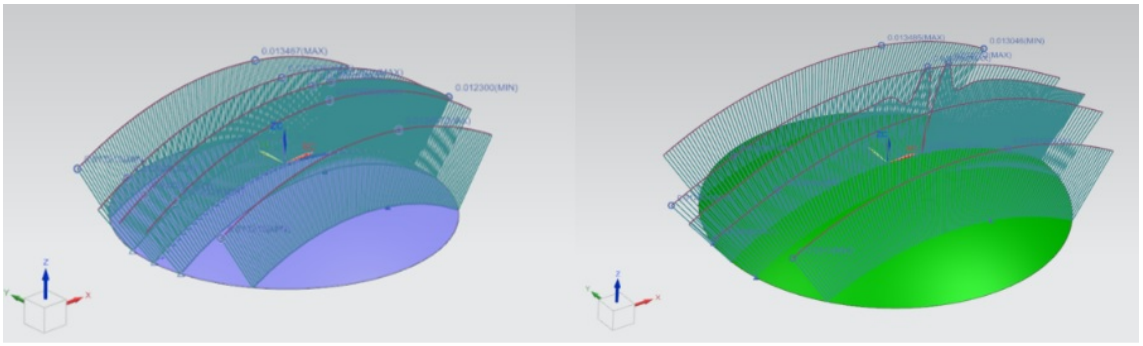

Figure 9. Simulation results monitor the changes on the free-form element sections. Example of DF influence simulation on the left, example of SF influence simulation on the right.

From the simulation results, it was evident that the deformation factor (DF) had a fundamental influence. When the DF grew from 1 to 1.5, the shape deviation grew from 3.3 µm up to 30.6 µm (i.e., almost 10 times) and the difference in the curvature of the surface also grew from the original 0.06 µm approx. 5.5 times to 0.34 µm. Additionally, when a coarser distance tolerance (DT) of 0.01 mm was used, an increase in curvature deviation of 0.62 µm and, on the contrary, a lower maximum shape deviation of 0.76 µm were achieved compared with the DT setting of 0.001. Thus, the DT setting did not have a significant influence on the surface shape changes. Finally, increasing the smoothing factor (SF) value (from 0 to 0.2) resulted in a slight decrease of the curvature deviation (by 0.027 µm). However, the maximum shape deviation of the surface quadrupled, from the original 3.3 µm to 13.5 µm.

Based on the simulation results, the DF of 1.0, DT of 0.001, and SF of 0.0 settings were chosen for the calculation of the global deformation function. The data obtained (see figure 10) were then imported to NX CAM as a `.prt` file and used for the corrective grinding experiment.

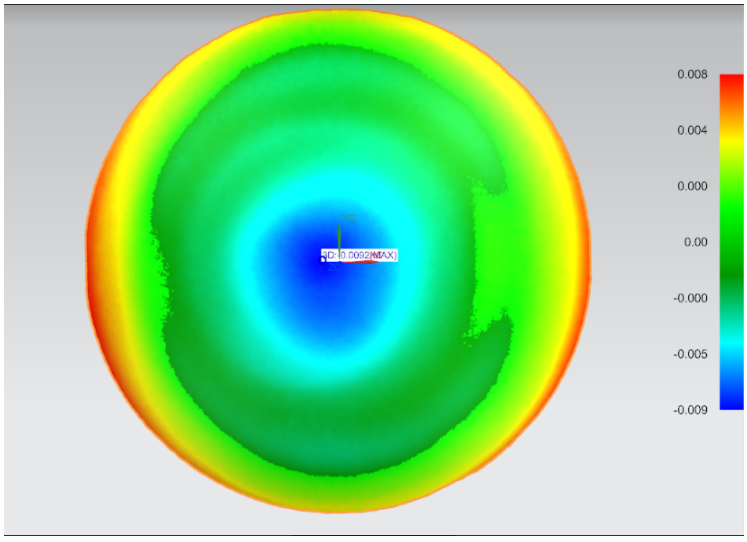

Figure 10. NX global deformation function used for corrective grinding.

2023 JINST 18 P04022

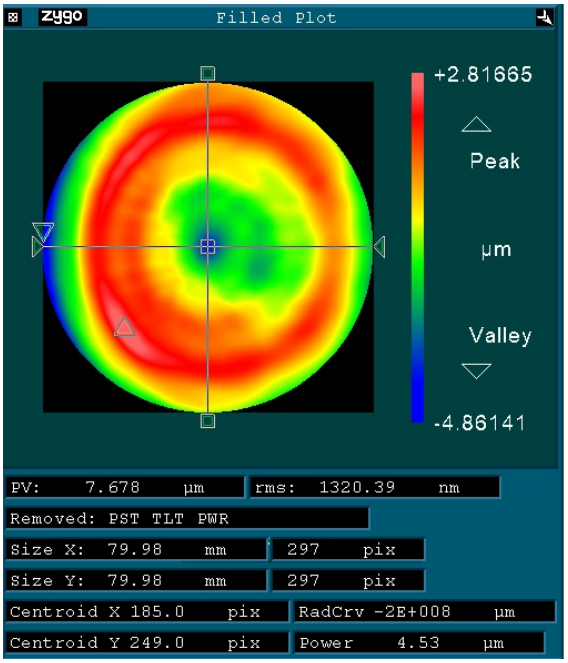

Figure 11. Free-form surface error after corrective grinding and pre-polishing; piston and tilt removed. Results from QED ASI.

The results of the corrective grinding experiment are presented in figure 11. A certain idea about the effect of corrective grinding on the individual components of the shape error can be obtained by applying the standard ISO 10110-5 surface error analysis (table 2). When comparing the surface error before and after corrective grinding, it is possible to see a significant reduction of the free-form surface radius error (SAG), contributing to the reduction of the PV value from 15 µm to 9 µm, probably due to the chosen DF global deformation function parameter setting, but barely affecting the surface curvature and residual error (IRR, RSI), which cannot be influenced to the required extent by the setting of the DT or SF parameters.

Table 2. ISO 101 10-5 analysis of the free-form surface error before and after corrective grinding.

ISO 101 10-5 parameter	Before corrective grinding	After corrective grinding
Sagital error SAG (µm PV)	8.8	5.5
Irregularity IRR (µm PV)	8.2	7.2
Residual error RSI (µm PV)	5.0	4.1

Even though the global deformation function in the used setting was not able to significantly suppress the IRR and RSI components of the shape error, it was possible, with the help of a single iteration of this corrective grinding, to achieve a shape error of less than 10 µm, which can be considered a suitable value for starting the polishing process.

Finally, the tool path calculated for corrective grinding was applied to the machining of two other free-forms, where the resulting surface eror was 9.6 and 7.9 µm PV, which means a variance of approximately 20% and can be considered as an indication of the process stability range.

2023 JINST 18 P04022

4 Conclusions

Based on the performed experiment, a CAD/CAM grinding process chain was developed and tested for the realization of precise optical free-form elements made of S-BSL7 optical glass with the required shape error of less than 10 µm after grinding. The free-form optical element machining was realized using the SolidWorks CAD software for construction, the Siemens NX software for grinding process programming, and the Satisloh SPM60 CNC machine equipped with post-processing software for the grinding itself. This chain, after solving the partial issues associated with the correct setting of the coordinate systems employed, with the tool kinematics, and with the necessary data handling, proved to be applicable for both conventional and corrective grinding. The resulting free-form element shape error was around 15 µm PV (2.6 µm RMS) for conventional grinding and approximately 9 µm PV (1.9 µm RMS) for corrective grinding performed by the global deformation function. Results achieved by the application of this corrective grinding to machining other free-forms varied by approximately 20%, which can be perceived as an indication of the process stability range. In any case, the results represent a sufficient shape accuracy to allow subsequent polishing with the realistic goal of achieving the final shape accuracy in the order of units of optical fringes.

Acknowledgments

This ESA-funded activity is carried out within the framework of the Technology Development Element "New Optical Polishing Techniques for Aspherical and Free Form Lenses" project (ESA Contract No. 4000134543/21/NL/AR) and the "Partnership for Excellence in Superprecise Optics" project (Reg. No. CZ.02.1.01/0.0/0.0/16_026/0008390) and co-funded from European Structural and Investment Funds.

References

[1] O. Fähnle, *Process optimization in optical fabrication*, *Opt. Eng.* **55** (2016) 035106.

[2] M. Bass, *Handbook of Optics. Volume II. Design, Fabrication, and Testing; Sources and Detectors; Radiometry and Photometry*, 3rd edition, McGraw-Hill Professional, New York, NY, U.S.A. (2010) [ISBN: 9780071498906] and online at https://www.accessengineeringlibrary.com/content/book/9780071498906.

[3] A. Lasemi, D. Xue and P. Gu, *Recent development in CNC machining of freeform surfaces: A state-of-the-art review*, *Comput.-Aided Des.* **42** (2010) 641.

[4] E. Wagner, *A New Optimization CAD/CAM/CAE Technique for the Processing of the Complex* 3*D Surfaces on* 5 *Axes CNC Machines*, *Procedia Technol.* **19** (2015) 34.

[5] International Organization for Standardization, *Automation systems and integration. Numerical control of machines. Program format and definitions of address words. Part 1. Data format for positioning, line motion and contouring control systems*, ISO 6983-1:2009 (2009) and online at https://www.iso.org/standard/34608.html.

[6] T. Dodok, N. Čuboňová, M. Císar, I. Kuric and I. Zajačko, *Utilization of Strategies to Generate and Optimize Machining Sequences in CAD/CAM*, *Procedia Eng.* **192** (2017) 113.

2023 JINST 18 P04022

[7] N. Vukašinović and J. Duhovnik, *Introduction to Freeform Surface Modelling*, in *Advanced CAD Modeling*, *Springer Tracts in Mechanical Engineering*, Springer, Cham, Switzerland (2019), pp. 1–48 [DOI:10.1007/978-3-030-02399-7_1].

[8] P. Murphy, G. Forbes, J. Fleig, P. Dumas and M. Tricard, *Stitching Interferometry: A Flexible Solution for Surface Metrology*, *Opt. Photonics News* **14** (2003) 38.

[9] S. Chen, S. Xue, D. Zhai and G. Tie, *Measurement of Freeform Optical Surfaces: Trade-Off between Accuracy and Dynamic Range*, *Laser Photonics Rev.* **14** (2020) 1900365.

[10] International Organization for Standardization, *Optics and photonics. Preparation of drawings for optical elements and systems. Part 19. General description of surfaces and components*, ISO 10110-19:2015 (2015) and online at https://www.iso.org/standard/60467.html.

[11] F.Z. Fang, X.D. Zhang, A. Weckenmann, G.X. Zhang and C. Evans, *Manufacturing and measurement of freeform optics*, *CIRP Annals* **62** (2013) 823.

[12] F.L. Wolfs, J. Ross and S. DeFisher, *Advances in freeform manufacturing*, in *Optifab 2019*, proceedings of the *SPIE Optifab*, Rochester, New York, U.S.A, 14–17 October 2019, B.L. Unger and J.D. Nelson eds., SPIE (2019) [*Proc. SPIE* **11175** (2019) 1117511].

2023 JINST 18 P04022